Nuclear Structure Towards $N = 40$ ^{60}Ca: In-Beam γ-Ray Spectroscopy of ^{58,60}Ti

A. Gade,[1,2] R. V. F. Janssens,[3] D. Weisshaar,[1] B. A. Brown,[1,2] E. Lunderberg,[1,2] M. Albers,[3] V. M. Bader,[1,2] T. Baugher,[1,2] D. Bazin,[1] J. S. Berryman,[1] C. M. Campbell,[4] M. P. Carpenter,[3] C. J. Chiara,[5,3] H. L. Crawford,[4,*] M. Cromaz,[4] U. Garg,[6] C. R. Hoffman,[3] F. G. Kondev,[7] C. Langer,[1,8] T. Lauritsen,[3] I. Y. Lee,[4] S. M. Lenzi,[9] J. T. Matta,[6] F. Nowacki,[10] F. Recchia,[1,†] K. Sieja,[10] S. R. Stroberg,[1,2] J. A. Tostevin,[11] S. J. Williams,[1] K. Wimmer,[12,1] and S. Zhu[3]

[1]*National Superconducting Cyclotron Laboratory, Michigan State University, East Lansing, Michigan 48824, USA*
[2]*Department of Physics and Astronomy, Michigan State University, East Lansing, Michigan 48824, USA*
[3]*Physics Division, Argonne National Laboratory, Argonne, Illinois 60439, USA*
[4]*Nuclear Science Division, Lawrence Berkeley National Laboratory, Berkeley, California 94720, USA*
[5]*Department of Chemistry and Biochemistry, University of Maryland, College Park, Maryland 20742, USA*
[6]*Department of Physics, University of Notre Dame, Notre Dame, Indiana 46556, USA*
[7]*Nuclear Engineering Division, Argonne National Laboratory, Argonne, Illinois 60439, USA*
[8]*Joint Institute for Nuclear Astrophysics, Michigan State University, East Lansing, Michigan 48824, USA*
[9]*Dipartimento di Fisica e Astronomia dell'Università and INFN, Sezione di Padova, I-35131 Padova, Italy*
[10]*IPHC, IN2P3-CNRS et Université de Strasbourg, F-67037 Strasbourg, France*
[11]*Department of Physics, Faculty of Engineering and Physical Sciences, University of Surrey, Guildford GU2 7XH, United Kingdom*
[12]*Department of Physics, Central Michigan University, Mt. Pleasant, Michigan 48859, USA*

(Received 31 December 2013; published 21 March 2014)

Excited states in the neutron-rich $N = 38$, 36 nuclei ^{60}Ti and ^{58}Ti were populated in nucleon-removal reactions from ^{61}V projectiles at 90 MeV/nucleon. The γ-ray transitions from such states in these Ti isotopes were detected with the advanced γ-ray tracking array GRETINA and were corrected event by event for large Doppler shifts ($v/c \sim 0.4$) using the γ-ray interaction points deduced from online signal decomposition. The new data indicate that a steep decrease in quadrupole collectivity occurs when moving from neutron-rich $N = 36$, 38 Fe and Cr toward the Ti and Ca isotones. In fact, ^{58,60}Ti provide some of the most neutron-rich benchmarks accessible today for calculations attempting to determine the structure of the potentially doubly magic nucleus ^{60}Ca.

DOI: 10.1103/PhysRevLett.112.112503 PACS numbers: 23.20.Lv, 21.60.Cs, 27.30.+t, 29.38.Db

One of the main goals of nuclear physics is the development of a predictive model for the properties of all nuclei, including the shortest-lived species in as yet unexplored regions of the nuclear chart. This is important, for example, in the quest to understand the origin of the elements in the Universe since many nucleosynthesis processes involve nuclei far removed from the valley of β stability. One of the cornerstones in the description of nuclear properties is nuclear shell structure—whereby discrete nucleon single-particle orbitals are clustered in energy, resulting in stabilizing energy gaps occurring for certain "magic" proton or neutron numbers. Doubly magic nuclei, with both proton and neutron magic numbers, are particularly important for the development of nuclear models as they serve as essentially inert cores, reducing the many-body problem to that of the set of "valence nucleons" outside this core. However, modifications of shell structure have already been observed in short-lived nuclei with extreme neutron-to-proton ratios, with new shell gaps developing and some of the canonical magic numbers disappearing [1–4]. Considerable experimental and theoretical efforts are aimed at describing the physics driving such changes which are revealed most clearly on the neutron-rich side of the nuclear chart.

Data for chains of proton-magic isotopes and regions of rapid shell evolution offer (complementary) challenging tests of nuclear models, allowing changes in nuclear structure to be tracked as a function of isospin and providing demanding benchmarks for calculations incorporating new physics effects. The chain of Ca isotopes (with magic proton number $Z = 20$) and the region of neutron-rich nuclei near $N = 40$, which are subject to rapid shell and shape changes [5–9], coincide at ^{60}Ca. In addition to the first spin–orbit driven neutron subshell closure at $N = 28$ ^{48}Ca, the neutron-rich Ca isotopes exhibit two additional subshell gaps at $N = 32$ [10] and $N = 34$ [11], attributed in part to the action of the monopole parts of the proton-neutron tensor force in the regime of large neutron excess [12,13].

Nothing is known experimentally about the properties of the most neutron-rich $N = 40$ isotones ^{62}Ti and ^{60}Ca. While the existence of ^{62}Ti has been established [14], ^{60}Ca has not yet been observed. In fact, the position of the neutron drip line in Ca appears to depend sensitively on both the location of the neutron $1g_{9/2}$ orbital, which starts to be filled at $N = 40$ in ^{60}Ca, and a variety of correlations and many-body effects [15,16]. Calculations with realistic two- and three-body forces [17,18] predict the neutron drip

line to be located around ^{60}Ca, while many mean-field and density-functional theories have the Ca isotopes (at least those with even A) bound out to $A = 68$–76 [19]. The relativistic continuum Hartree-Bogoliubov approach of Meng *et al.* [15] has the neutron $1g_{9/2}$ and $3s_{1/2}$ orbitals unbound, but correlation effects, predominantly pairing, bind even-A Ca out to $A = 72$, while the SkM* Skyrme functional has the neutron $1g_{9/2}$ orbital bound and predicts the Ca drip line to be at $A = 70$ [15]. Clearly, information on the structure of neutron-rich nuclei with $A \approx 60$ is important to help benchmark modern calculations which differ in their prediction of the location of the Ca drip line by more than 10 mass units. The calculations of Ref. [20] suggest that the regime of weak binding applying to ^{60}Ca leads to intriguing consequences, such as the presence of a halo structure and of two Efimov states in ^{62}Ca.

The first spectroscopy of ^{60}Ti and the identification of new γ-ray transitions in ^{58}Ti are reported here. At present, $^{60}_{22}\mathrm{Ti}_{38}$ is probably the nucleus closest to $^{62}_{22}\mathrm{Ti}_{40}$ and $^{60}_{20}\mathrm{Ca}_{40}$ that can be studied until next-generation rare-isotope facilities come online. The measurements were enabled by the luminosity inherent to fast fragmentation-beam measurements [3] and the efficiency and spectral quality provided by the advanced γ-ray tracking array GRETINA [21].

Excited states in the neutron-rich Ti isotopes were populated in the ^{9}Be(^{61}V, ^{58,60}Ti $+ \gamma$)X nucleon removal reactions at 90.0 MeV/u at the Coupled Cyclotron Facility at NSCL. The ^{61}V ions were produced from a 140-MeV/u primary ^{82}Se beam impinging on a 423-mg/cm^2 ^{9}Be production target, and were separated using a 240-mg/cm^2 Al degrader in the A1900 fragment separator [22]. The momentum acceptance of the separator was restricted to 3%, yielding typical on-target rates of 15 ^{61}V/s. About 10% of the secondary beam was ^{61}V, with ^{62}Cr (32%) and ^{64}Mn (45%) being the most intense other components.

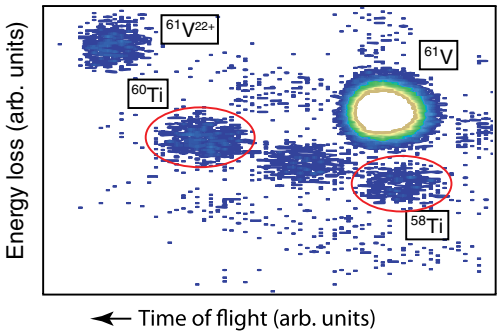

FIG. 1 (color online). Identification spectrum for the reaction residues produced in ^{9}Be(^{61}V, ^{A}Ti)X at a 90-MeV/u midtarget energy. All reaction residues are unambiguously identified by their energy loss, measured in the S800 ionization chamber, and their time of flight.

The secondary ^{9}Be reaction target (376 mg/cm^2 thick) was located at the target position of the S800 spectrograph [23]. Reaction products were identified on an event-by-event basis at the instrument's focal plane with the standard detection system [23]. The particle-identification spectrum for ^{58,60}Ti produced from incoming ^{61}V ions is presented in Fig. 1. The spectrograph was centered on the ^{60}Ti one-proton knockout residues while the ^{58}Ti momentum distribution was cut by the S800 acceptance. The inclusive cross section for one-proton knockout from ^{61}V to ^{60}Ti was measured to be $\sigma_{\mathrm{inc}} = 7.9(7)$ mb.

The high-resolution γ-ray detection system GRETINA [21], an array of 36-fold segmented high-purity Ge detectors, was used to measure the prompt γ rays emitted by the reaction residues. The seven GRETINA modules—with four crystals each—were arranged in two rings. Four modules were located at 58° and three at 90° with respect to the beam axis. Online signal decomposition provided γ-ray interaction points for event-by-event Doppler reconstruction of the photons emitted in flight at $v/c = 0.4$. The information on the momentum vector of projectilelike reaction residues, as reconstructed from ray tracing through the spectrograph, was incorporated in the Doppler reconstruction. Figure 2 presents these Doppler-reconstructed spectra for ^{58}Ti and ^{60}Ti with addback, a procedure correcting for scattering of photons from one crystal into a neighbor, included [24]. The high peak-to-background ratio enables spectroscopy to be performed at the low levels of statistics that are inherent to investigations of the most exotic nuclei.

In ^{58}Ti, in addition to the previously known $2^+_1 \rightarrow 0^+_1$ transition at 1047(4) keV [25,26], two additional γ rays could be identified at 991(4) and 619(5) keV. The reaction to ^{58}Ti is not a direct process and, typically, the population of yrast

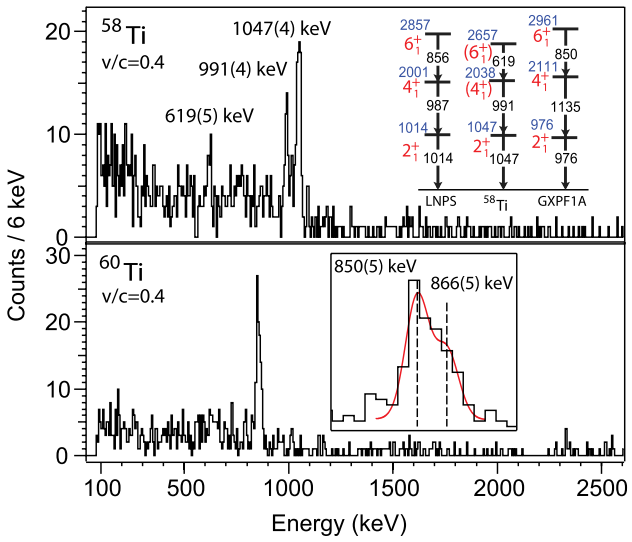

FIG. 2 (color online). Doppler-reconstructed γ-ray spectra in coincidence with ^{58,60}Ti reaction residues. The indication of a transition doublet in ^{60}Ti is shown as an inset in the lower panel.

states is favored in such fragmentation processes. Thus, based on the observed intensity pattern, the 991-keV γ ray is tentatively assigned as the $4_1^+ \rightarrow 2_1^+$ decay and it is suggested that the 619-keV line corresponds to the $6_1^+ \rightarrow 4_1^+$ transition. Evidence for the coincidence between the 991- and 1047-keV γ rays is discussed below. The inset shows that the two shell-model effective interactions for this region of the nuclear chart, LNPS [16] and GXPF1A [27], describe the proposed level scheme well although the neutron model spaces differ significantly with GXPF1A restricted to the neutron fp shell and LNPS including the neutron $d_{5/2}$ and $g_{9/2}$ orbitals in addition. The agreement is good with both interactions, suggesting that incorporating the $1g_{9/2}$ and $2d_{5/2}$ neutron orbitals may not be critical, in agreement with conclusions presented in Ref. [26]. Note that the present spin assignments are consistent with the fact that the 991- and 619-keV transitions were not observed by Ref. [26], since 4^+ and 6^+ states are not expected to be populated strongly in inelastic proton scattering.

In ^{60}Ti, a peak structure at 860 keV is observed on top of very little background. One-proton knockout is a direct reaction with sensitivity to the single-particle degrees of freedom and it offers insight into the overlap in structure between the projectile ground state and the final states populated in the knockout residue [28]. The partial cross section to an excited final state is determined from the efficiency-corrected peak area relative to the number of knockout residues. A GEANT4 simulation of the GRETINA setup [29], which reproduced the intensity of standard calibration sources, was used to model the in-beam full-energy peak efficiency of the detector array, including the Lorentz boost. The simulated in-beam efficiency was employed to extract intensities from the peak areas in ^{60}Ti. Assuming that the peak structure in ^{60}Ti corresponds to a single transition then implies that 111(12)% of the knockout proceeds to the state depopulated by this 860-keV transition and that there is essentially no population of any other final state in ^{60}Ti. For a nucleus bound by more than 5 MeV, this scenario appears to be rather unlikely.

In fact, the asymmetric peak shape at 860 keV supports the presence of a doublet (Fig. 2, inset). Analysis as a doublet suggests the presence of two γ rays at 850(5) and 866(5) keV, presumably corresponding to the $2_1^+ \rightarrow 0_1^+$ and $4_1^+ \rightarrow 2_1^+$ transitions in ^{60}Ti, associated with 40(10)% population of the 4_1^+ state, 30(11)% of the 2_1^+ level, and 29(12)% of the ground state and unobserved levels not feeding the proposed 2_1^+ or 4_1^+ states. GRETINA's $\gamma\gamma$ coincidence capability supports further examination of the proposed doublet. Figure 3(a) provides the total projection of the coincidence matrix for ^{60}Ti (upper panel) and the spectrum gated on the 860-keV peak (lower panel). Clearly, a peak in the same region (self-coincidence) and a corresponding Compton edge between 600–700 keV are visible. Similarly, in Fig. 3(b), the projection of the ^{58}Ti $\gamma\gamma$ coincidence matrix is given (upper panel) as is the spectrum

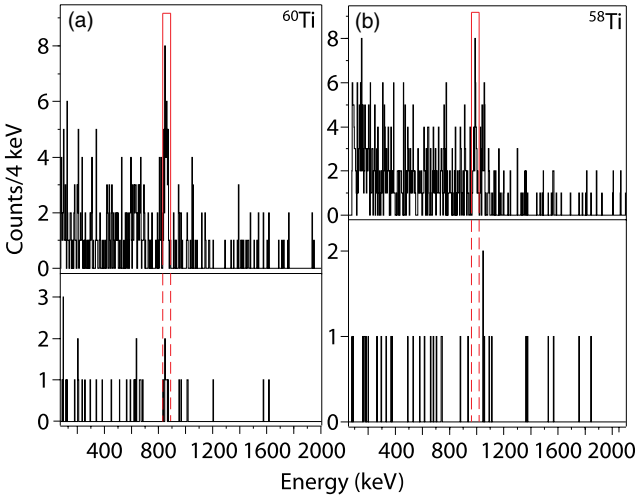

FIG. 3 (color online). Projections of the ^{60,58}Ti $\gamma\gamma$ coincidence matrices, nearest-neighbor addback included [24] (upper panels) and gated coincidence spectra (lower panels): (a) ^{60}Ti, the gate on the 860-keV peak returns a self-coincidence and Compton edge; (b) ^{58}Ti, the gate on the 991-keV transition shows no self-coincidence and returns the peak at 1047 keV, consistent with a 1047–991 keV cascade.

with a coincidence condition on the 991-keV transition (lower panel). No self-coincidence events are visible; instead, the 1047-keV γ ray appears, confirming the 991–1047 keV cascade. Thus, the self-coincidence of the 860 keV peak structure is evidence for a coincident doublet of γ-ray transitions in ^{60}Ti.

Knockout calculations can be used for further guidance. The ground-state spin of ^{61}V is not known experimentally. Shell-model calculations with the LNPS effective interaction predict a $3/2^-$ ground state, in agreement with β-decay results [30]. The GXPF1A effective interaction [27], which does not include the potentially important neutron $d_{5/2}$ and $g_{9/2}$ orbitals, predicts a $7/2^-$ ground state with excited $5/2_1^-$ and $3/2_1^-$ levels within 400 keV. Using the one-nucleon knockout formalism detailed in Ref. [31], the GXPF1A and LNPS spectroscopic factors with respect to the ground state of ^{61}V, and assuming a reduction factor of $R_s \approx 0.5$ at a nucleon separation energy difference of the projectile of $S_n - S_p \approx -10$ MeV [31], the partial cross sections to bound final states in ^{60}Ti are calculated and confronted with experiment in Fig. 4. For the LNPS effective interaction, the calculated inclusive cross section agrees with the measurement, while the GXPF1A calculation predicts a slightly higher cross section. From the GXPF1A calculation, four excited levels, 4_1^+, 2_2^+, 4_2^+, and 6_1^+, should be populated strongly. There is no evidence in the spectrum for additional strong γ rays that would correspond to the respective transitions. Note that assuming a $5/2^-$ or $3/2^-$ ground state within the GXPF1A calculations always results in the strong population of three or more excited states, corresponding to the presence of

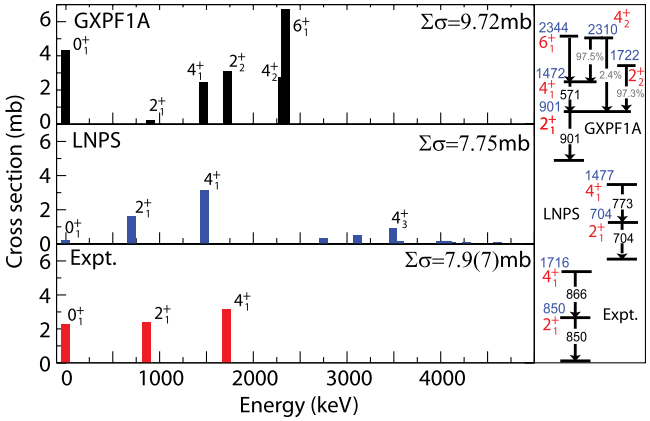

FIG. 4 (color online). Calculated and measured partial cross sections to final states in ^{60}Ti using GXPF1A and LNPS spectroscopic factors and the procedure outlined in the text. The experimental cross sections to the 2_1^+ and 4_1^+ states were deduced from the γ-ray intensities and the 0_1^+ population results from subtraction. The so-determined strength constitutes 29 (12)%, 30(11)%, and 40(10)% population of the 0_1^+, 2_1^+, and 4_1^+ states, which will include unobserved feeding from higher-lying states that could not be observed due to the lack of statistics. (In Fig. 2, about 8 counts should be seen in the ^{60}Ti spectrum per 1 mb at 1.5 MeV.)

several strong γ-ray transitions in addition to the $2_1^+ \rightarrow 0_1^+$ and $4_1^+ \rightarrow 2_1^+$ decays (e.g., the $6_1^+ \rightarrow 4_1^+$, $2_2^+ \rightarrow 2_1^+$, or $4_2^+ \rightarrow 4_1^+$ transitions). With LNPS, the single-particle strength distribution resembles the data with the majority of the cross section carried by the 2_1^+ and 4_1^+ states. Discrepant is the 29(12)% population deduced for the ground state by subtraction. However, the experimental strength to the ground state will also include unobserved feeding from higher excited levels that bypass the 2_1^+ and 4_1^+ states and will act as a funnel for a fraction of the strength predicted to be fragmented over higher-lying states. Unlike for the ^{60}Ti excitation energies, which do not signal a clear difference between the predictions for the different model spaces, the spectroscopic strengths clearly indicate that the neutron $d_{5/2}$ and $g_{9/2}$ orbitals are important for the description of the overlap of the ^{61}V ground state with the final-state wave functions in ^{60}Ti.

Over the past decade, with advances in nuclear experiment, the neutron-rich Cr and Fe nuclei around $N = 40$ were found to be strongly deformed, presenting a challenging testing ground for the theoretical modeling of shell evolution. The next experimental and theoretical key benchmark is the understanding of the neighboring $N = 2Z$ nucleus ^{60}Ca. As shown in Fig. 1 of Ref. [16], the $N = 40$ shell gap computed with the LNPS interaction vanishes as $Z = 20$ (calcium) is approached, and the ground state of ^{60}Ca is dominated by four-particle–four-hole ($4p$-$4h$) neutron excitations from the pf shell into the $g_{9/2}$-$d_{5/2}$ orbitals (Table I in Ref. [16]). However, the shell-model extrapolation of single-particle energies is often not accurate [32], perhaps due to the lack of inclusion of three-body forces. Another approach would be to use Hartree-Fock or energy-density-functional calculations to estimate the $N = 40$ subshell gap. The 12 CSkP Skyrme functionals, used in Ref. [33], give a shell gap between the neutron $f_{5/2}$ and $g_{9/2}$ orbitals varying between 3 and 4 MeV at $Z = 20$. If the shell gap were this large, the ground state of ^{60}Ca would be dominated by $0p$-$0h$ rather than $4p$-$4h$ configurations. Clearly, the size of the $N = 40$ shell gap is crucial for the properties of nuclei in this region. Collective nuclei, such as ^{64}Cr, are in the "island of inversion" [16] because of strong quadrupole correlations for *both* protons and neutrons. With a large shell gap, there would be a dramatic change from a deformed to a spherical shape as one approaches $Z = 20$, since the protons encounter a spin-orbit (LS) closed shell with no available low-lying proton quadrupole excitations.

Shell-model calculations with the LNPS interaction provide a good description of the data in this region. In the case of ^{60}Ti, the excitation energies of both states are underestimated (2_1^+ energy by 150 keV and the 4_1^+ one by 240 keV). Since this nucleus is one of the farthest extrapolation points with no data available previously, it is interesting to study its sensitivity to modifications of the interaction and the resulting impact on the calculated structure of this region. Such modifications to the LNPS effective interaction—based on available, independent data in this region—are under way and offer the opportunity to assess the role of ^{60}Ti. With an increase of the $d_{5/2}$ single-particle energy by 250 keV and repulsion of $g_{9/2}$, $d_{5/2}$ monopole matrix elements by 200 keV, the description of the excitation energies of ^{60}Ti improves, with the 2_1^+ state calculated at 803 and the 4_1^+ level at 1609 keV. While these modifications increase the small $N = 40$ gap at ^{60}Ca by only 250 keV, they significantly alter the nuclear structure of the region with markedly changed $2p$-$2h$ and $4p$-$4h$ contributions to the wave functions. In the original LNPS effective interaction, the ground state and 2_1^+ state of ^{60}Ti contain 27% of $2p$-$2h$ and 41% of $4p$-$4h$ and 15% of $2p$-$2h$ and 45% $4p$-$4h$ contributions, respectively. With the modifications that improve the agreement for the ^{60}Ti excitation energies, these contributions change to 36% of $2p$-$2h$ and 33% of $4p$-$4h$ and 21% of $2p$-$2h$, 39% of $4p$-$4h$ for the ground and 2_1^+ states, respectively. Confirmation of the size of the $N = 40$ shell gap and of the role of multiparticle-multihole configurations beyond ^{60}Ti will likely only come with the next generation of experiments measuring properties of nuclei even closer to ^{60}Ca combined with advances in nuclear theory such as improved effective shell-model interactions built on those developed currently.

In summary, first structural information on ^{60}Ti was obtained by taking advantage of the spectral quality and the γ-ray coincidence efficiency of GRETINA. The first 2_1^+ state of ^{60}Ti, at an energy of 850(5) keV, is located at almost

twice the excitation energy of the corresponding 2_1^+ level in the $N = 38$ isotone ^{62}Cr, herewith signaling a steep decrease in collectivity with Z and yet another sudden structural change near $N = 40$. For ^{58}Ti, candidates for the (4_1^+) and (6_1^+) levels are reported. The data on ^{60}Ti are consistent with a shell-model prediction using the LNPS effective interaction which allows for the largest neutron model space yet, while they disagree with calculations restricted to the neutron fp shell. The ^{60}Ti excitation energies were shown to be sensitive to the details of the effective interaction, with significant impact on the particle-hole contents of the state's wave functions. This in turn drives the nuclear structure in this region. With these considerations, ^{60}Ti represents an important benchmark, being one of the most neutron-rich systems from which to extrapolate towards ^{60}Ca, a nucleus with an intrinsic structure closely tied to the location of the neutron drip line in the crucial semimagic Ca isotopic chain.

GRETINA was funded by the DOE, Office of Science. Operation of the array at NSCL was supported by NSF under Cooperative Agreement No. PHY-1102511 (NSCL) and DOE under Grant No. DE-AC02-05CH11231 (LBNL). We further acknowledge DOE Contract No. DE-AC02-06CH11357 (ANL) and Grant Nos. DE-FG02-94-ER40834 (UM) and DE-FG02-08ER41556 (NSCL) and support from NSF Grant Nos. PHY-1068217 (NSCL) and PHY-1068192 (ND). J. A. T. acknowledges support from the Science and Technology Facilities Council (U.K.) Grant No. ST/J000051. We are grateful for Augusto Macchiavelli's support of the GRETINA campaign at NSCL.

*Permanent address: Institute of Nuclear and Particle Physics, and Department of Physics and Astronomy, Ohio University, Athens, OH 45701, USA.

†Present address: Dipartimento di Fisica e Astronomia "Galileo Galilei," Università degli Studi di Padova, I-35131 Padova, Italy.

[1] T. Otsuka, Phys. Scr. **T152**, 014007 (2013).
[2] O. Sorlin and M.-G. Porquet, Prog. Part. Nucl. Phys. **61**, 602 (2008).
[3] A. Gade and T. Glasmacher, Prog. Part. Nucl. Phys. **60**, 161 (2008).
[4] R. V. F. Janssens, Nature (London) **459**, 1069 (2009).
[5] O. Sorlin *et al.*, Eur. Phys. J. A **16**, 55 (2003).
[6] E. Caurier, F. Nowacki, and A. Poves, Eur. Phys. J. A **15**, 145 (2002).
[7] P. Adrich *et al.*, Phys. Rev. C **77**, 054306 (2008).
[8] A. Gade *et al.*, Phys. Rev. C **81**, 051304(R) (2010).
[9] M. P. Carpenter, R. V. F. Janssens, and S. Zhu, Phys. Rev. C **87**, 041305(R) (2013).
[10] J. I. Prisciandaro *et al.*, Phys. Lett. B **510**, 17 (2001); A. Gade *et al.*, Phys. Rev. C **74**, 021302(R) (2006); D.-C. Dinca *et al.*, Phys. Rev. C **71**, 041302(R) (2005).
[11] R. V. F. Janssens *et al.*, Phys. Lett. B **546**, 55 (2002); S. N. Liddick *et al.*, Phys. Rev. Lett. **92**, 072502 (2004); D. Steppenbeck *et al.*, Nature (London) **502**, 207 (2013).
[12] T. Otsuka, R. Fujimoto, Y. Utsuno, B. A. Brown, M. Honma, and T. Mizusaki, Phys. Rev. Lett. **87**, 082502 (2001).
[13] T. Otsuka, T. Suzuki, R. Fujimoto, H. Grawe, and Y. Akaishi, Phys. Rev. Lett. **95**, 232502 (2005).
[14] O. B. Tarasov *et al.*, Phys. Rev. C **80**, 034609 (2009); O. B. Tarasov *et al.*, Phys. Rev. Lett. **102**, 142501 (2009).
[15] J. Meng, H. Toki, J. Y. Zeng, S. Q. Zhang, and S.-G. Zhou, Phys. Rev. C **65**, 041302(R) (2002).
[16] S. M. Lenzi, F. Nowacki, A. Poves, and K. Sieja, Phys. Rev. C **82**, 054301 (2010).
[17] G. Hagen, M. Hjorth-Jensen, G. R. Jansen, R. Machleidt, and T. Papenbrock, Phys. Rev. Lett. **109**, 032502 (2012).
[18] J. D. Holt, T. Otsuka, A. Schwenk, and T. Suzuki, J. Phys. G **39**, 085111 (2012).
[19] J. Erler, N. Birge, M. Kortelainen, W. Nazarewicz, E. Olsen, A. M. Perhac, and M. Stoitsov, Nature (London) **486**, 509 (2012).
[20] G. Hagen, P. Hagen, H.-W. Hammer, and L. Platter, Phys. Rev. Lett. **111**, 132501 (2013).
[21] S. Paschalis *et al.*, Nucl. Instrum. Methods Phys. Res., Sect. A **709**, 44 (2013).
[22] D. J. Morrissey, B. M. Sherrill, M. Steiner, A. Stolz, and I. Wiedenhoever, Nucl. Instrum. Methods Phys. Res., Sect. B **204**, 90 (2003).
[23] D. Bazin, J. A. Caggiano, B. M. Sherrill, J. Yurkon, and A. Zeller, Nucl. Instrum. Methods Phys. Res., Sect. B **204**, 629 (2003).
[24] D. Weisshaar *et al.* (to be published).
[25] N. Aoi *et al.*, Nucl. Phys. **A805**, 400c (2008).
[26] H. Suzuki *et al.*, Phys. Rev. C **88** 024326 (2013).
[27] M. Honma, T. Otsuka, B. A. Brown, and T. Mizusaki, Phys. Rev. C **65**, 061301(R) (2002); Eur. Phys. J. A **25**, 499 (2005).
[28] J. A. Tostevin, J. Phys. G **25**, 735 (1999); P. G. Hansen, and J. A. Tostevin, Annu. Rev. Nucl. Part. Sci. **53**, 219 (2003).
[29] L. A. Riley, UCGretina GEANT4, Ursinus College (unpublished).
[30] L. Gaudefroy *et al.*, Eur. Phys. J. A **23**, 41 (2005).
[31] A. Gade *et al.*, Phys. Rev. C **77**, 044306 (2008).
[32] B. A. Brown, Prog. Part. Nucl. Phys. **47**, 517 (2001).
[33] B. A. Brown, Phys. Rev. Lett. **111**, 232502 (2013).